



Ultrasound and the Biceps Tendon: Diagnostic and Therapeutic Benefits

4

Ashley J. Bassett, Levon N. Nazarian,
and Michael G. Ciccotti

Introduction

The biceps brachii is a biarticular muscle that plays a pivotal role in shoulder and elbow function. It originates proximally at the scapula and inserts distally in the forearm at the tuberosity of the proximal radius, spanning both the shoulder and elbow joints. The biceps brachii is a powerful elbow flexor and forearm supinator composed of two distinct heads and three tendons. Injury to the long head of biceps tendon can arise from acute or chronic tensile overload, mechanical impingement, and tendon instability and/or secondary to various inflammatory or degenerative shoulder conditions. Long head of biceps tendon pathology is often associated with concomitant rotator cuff and/or labral injury [1]. Distally, biceps tendon injury may result from a combination of chronic processes, including mechanical impingement and

diminished tendon vascularity, or from an acute traumatic tensile overload. Imaging options for proximal and distal biceps brachii pathology include sonography and magnetic resonance imaging.

The use of sonography (US) for the evaluation and treatment of various musculoskeletal disorders has risen dramatically over the past decade, likely related to a multitude of factors. Sonography is a unique imaging modality that permits dynamic soft tissue evaluation, lacks radiation exposure, enables patient interaction during the examination, and offers immediate comparison with the contralateral limb. Technologic advancements have led to higher-resolution images, decreased equipment costs, and improved portability. New patient safety initiatives coupled with an increasing emphasis on cost reduction in healthcare have also contributed to the growing popularity of US [2–4].

Musculoskeletal US employs high-frequency sound waves to image soft tissue structures. Sonography can readily identify and differentiate tendons, muscles, ligaments, nerves, and vessels at a spatial resolution of approximately 0.1 mm; this has established US as a prime diagnostic tool for the evaluation of shoulder and upper extremity pathology [2, 3]. In addition to diagnostic capabilities, US is often used to guide therapeutic interventions including aspiration, injection, tenotomy, release, and hydrodissection [5]. This

A. J. Bassett (✉)
The Orthopedic Institute of New Jersey,
Sparta, NJ, USA

L. N. Nazarian
Thomas Jefferson University, Department of
Radiology, Philadelphia, PA, USA
e-mail: Levon.Nazarian@jefferson.edu

M. G. Ciccotti
Rothman Orthopaedic Institute, Thomas Jefferson
University, Department of Orthopaedic Surgery,
Philadelphia, PA, USA
e-mail: michael.ciccotti@rothmanortho.com

chapter will focus on diagnostic and interventional US for the evaluation and treatment of biceps brachii pathology.

Anatomy of the Biceps Brachii

Knowledge of the biceps brachii anatomy and normal morphologic variants is critical to interpret US images and recognize pathology. The short head of the biceps brachii (SHB) originates from the coracoid process of the scapula and together with the coracobrachialis is known as the conjoint tendon. The long head of the biceps brachii (LHB) originates from the supraglenoid tubercle of the scapula and the superior labrum, most often from the posterior aspect of the superior labrum [6]. The intraarticular portion of the LHB tendon courses over the anterosuperior portion of the humeral head and then passes beneath the coracohumeral ligament (CHL) and through the rotator interval between the supraspinatus and subscapularis tendons.

Within the rotator interval, the superior glenohumeral ligament (SGHL), located deep to the LHB tendon, blends with the CHL superficial to the LHB tendon to form a medial U-shaped sling. As the tendon angles sharply toward the entrance of the bicipital groove, superficial and deep fibers of the subscapularis and supraspinatus tendons join with the SGHL/CHL complex to form the *biceps reflective pulley*, stabilizing the LHB tendon in the rotator interval and proximal groove [7]. Within the bicipital groove of the humerus, the tendon is surrounded by a sheath formed by extension of the glenohumeral joint synovium. Along the course of the bicipital groove, the LHB tendon is stabilized by an intricate network of fibers from the supraspinatus, subscapularis, and CHL that span between the greater and lesser tuberosities of the humerus. Continuation of these fibers blends to form the *transverse humeral ligament (THL)*. Anatomic studies have shown the THL is located at the distal extent of the bicipital groove and plays a less significant role in LHB tendon stability than previously thought [8]. Rather, integrity of biceps reflective pulley and the supraspinatus and subscapularis tendons

appear to be most important for stability of the biceps within the groove. Injury to one or more soft tissue components of the biceps pulley can result in biceps tendon instability and ensuing attritional tendinopathy. Beyond the bicipital groove, the LHB tendon blends into its muscle belly at the upper myotendinous junction located deep to the pectoralis major tendon. After emerging distal to the inferior border of the pectoralis major, the long head of the biceps brachii gradually coalesces with the short head of the biceps brachii at the level of the deltoid tuberosity.

Though interdigitation occurs between the long head and short head of the biceps brachii, both muscle bellies contribute individually to form distinct portions of the distal biceps tendon, roughly 7 cm above the level of the elbow joint. The distal biceps tendon is a flat paratenon-lined extrasynovial structure with no tendon sheath. Coursing distally, it spirals approximately 90°, moving from medial to lateral and superficial to deep. The distal biceps tendon enters the antecubital fossa and inserts onto the tuberosity of the proximal radius over an area of 3 cm² in a semi-lunar footprint. Fibers from the short head of the biceps brachii attach distally and slightly anteriorly at the radial tuberosity and contribute mostly to elbow flexion. Fibers from the long head of the biceps brachii attach proximally and slightly posteriorly and act as a powerful supinator [9].

There are two bursae that surround the distal biceps tendon as it approaches the radial tuberosity that can become inflamed and filled with fluid. The *bicipitoradial bursa* lies between the distal biceps tendon and the anterior aspect of the radial tuberosity and functions to decrease friction between the two structures with forearm pronation and supination. The *interosseous bursa* contacts the interosseous membrane and lies medial to the bicipitoradial bursa and the insertion of the distal biceps tendon [10]. At the distal musculotendinous junction, a thin fibrous structure known as the *lacertus fibrosus* or *bicipital aponeurosis* arises from the tendon and extends medially across the antecubital fossa, protecting the median nerve and brachial artery, and blends with the antebrachial fascia covering the superficial forearm flexors. An intact lacertus fibrosus is

thought to contribute to elbow flexion and forearm supination and may also limit tendon retraction in cases of complete distal biceps tendon rupture [11].

Morphologic variations of the biceps brachii are common. The origin of the LHB tendon exhibits normal variability with the most common pattern of origin consisting of fibers arising from the supraglenoid tubercle and the posterior labrum [12]. Attachments to the anterior and superior labrum have also been described. The LHB can appear as a bifurcate tendon with two tendon limbs arising from a single biceps tendon origin [13]. Congenital absence of the long head is rare but has been associated with glenohumeral instability and impingement [12]. Lastly, supernumerary heads may be present in 9–22% of the population with the highest incidence in Japanese, South African, and Colombian ethnicities [14]. Accessory fascicles most commonly arise from the humeral shaft, termed the *humeral head of the biceps brachii*. Additional fascicles can also arise from the glenohumeral joint capsule and tuberosities of the humerus [15]. Distally, the biceps tendon is often two distinct tendons, each a continuation of the long and short heads of the biceps brachii muscle. While the distal biceps tendon often appears as one tendon on imaging, appearance of a bifurcate tendon is a normal anatomic variant and should be recognized as such. The tendon is also wider and thicker at the level of the radial tuberosity in males compared to females [9]. Additionally, the distal biceps tendon may have slips extending to the medial epicondyle, medial intermuscular septum, pronator teres, or extensor carpi radialis brevis muscles [16].

Basics of Musculoskeletal Sonography

Before focusing on the utility of US for biceps brachii pathology, it is first essential to understand fundamental principles of musculoskeletal US, including the necessary equipment, basic definitions, and the normal appearance of various tissues and anatomic structures. Sonography requires an ultrasound machine, a transducer or

probe attached to the body of the device, and coupling gel. The transducer contains a linear or curvilinear array of thin crystals that produce a high-frequency sound wave through the transformation of electrical energy into mechanical energy, a process termed *piezoelectricity*. The electrical system of the machine transmits a rapidly alternating current to the transducer crystals, causing them to vibrate and generate a sinusoidal ultrasound wave. The sound wave is then transmitted to the tissue through US coupling gel. Gray-scale US images are generated based on the amount of reflection and absorption of the ultrasound waves by the various tissues being imaged and the interfaces between them. Reflected sound waves are detected by the transducer, transformed back into an electrical signal, and translated into an image.

The amplitude and frequency of the ultrasound wave are determined by the amplitude and frequency of the electrical current; however, the material properties and thickness of the piezoelectric crystals impact the range of frequencies that the transducer can produce. This is important to consider when selecting an ultrasound transducer, as higher-frequency sound waves (>10 MHz) generate higher-resolution images with superior spatial resolution (<1 mm). However, high-frequency ultrasound waves also have limited penetration depth. While most musculoskeletal structures being imaged on ultrasound are relatively superficial and therefore well-visualized with a high-frequency transducer, deeper structures, such as the hip joint, may require use of a medium-frequency transducer (5–8 MHz) for optimal evaluation.

Musculoskeletal US utilizes frequencies in the range of 10–17 MHz or greater to generate images of osseous and soft tissue structures based on their unique composition, density, and stiffness. Bodily tissues have different *acoustic impedance* values based on the tissue density and sound wave velocity. The acoustic impedance describes the amount of resistance an ultrasound wave encounters as it passes through the tissue and relates to the fraction of ultrasound wave energy reflected and, thereby, the tissue echogenicity. Dense tissue (i.e., bone) has a larger

acoustic impedance value with greater resistance to ultrasound wave propagation, resulting in a large amount of energy reflection that manifests as a bright white structure on the US image. Conversely, low-density tissue (i.e., blood) has a smaller acoustic impedance value with less resistance to sound wave penetration, leading to more energy absorbed and less reflected, producing a darker structure on the US image. Sound wave reflections occur at the interface between tissues of differing density or stiffness, termed an *acoustic interface*. The greater the difference in acoustic impedance between the two tissue types, the more ultrasound wave energy is reflected at the interface, generating a brighter border on US image.

Understanding the expected US features of different musculoskeletal tissues is helpful for identifying and differentiating normal anatomic structures. Tissue appearance is generally described by echogenicity, echotexture, compressibility, and blood flow on Doppler examination. Tissue *echogenicity* is a measure of acoustic reflectance and is categorized as hyperechoic, isoechoic, hypoechoic, and anechoic. Hyperechoic tissues have a high percentage of reflection and manifest as bright white structures. Hypoechoic tissues have a lower percentage of reflection and appear darker. Isoechoic structures are similar in brightness to adjacent muscle, while anechoic materials exhibit little to no reflection and appear black. These terms can be used to characterize the US appearance of a structure alone (i.e., a normal tendon is often bright or hyperechoic) or in relation to surrounding structures (i.e., a tendon affected by tendinopathy is generally darker, or hypoechoic, compared to surrounding normal tendons). *Echotexture* refers to the internal pattern of sound wave reflection and depends on the orientation of the transducer relative to the structure. A *transverse view*, also called short axis view or axial view, is oriented perpendicular to the structure of interest and generates a cross-sectional image. A *longitudinal view*, also called a long axis view, is oriented parallel to the structure of interest. A nerve imaged longitudinally will exhibit a fas-

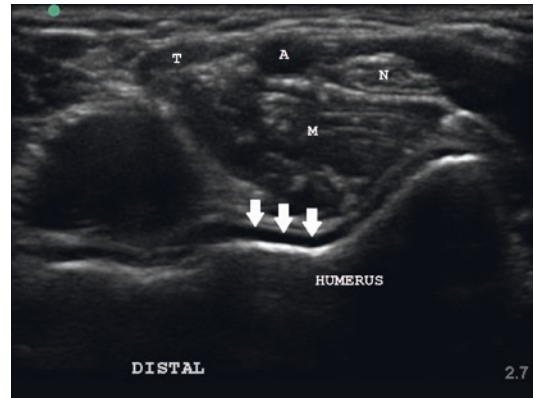


Fig. 4.1 Transverse view at the antecubital fossa shows the different echogenicity and echotexture of various anatomic structures. The median nerve (N) exhibits a mixed echogenicity honeycomb fascicular pattern. The brachial artery (A) just lateral to the nerve has a uniform anechoic appearance and is compressible. The distal biceps tendon (T) is characterized by a fibrillar pattern that is more tightly packed compared to the fascicular pattern of a nerve. The brachialis muscle (M) exhibits a “starry-night” pattern of loosely packed muscle fibers. The distal humerus bone has a smooth hyperechoic border with the overlying hyaline cartilage (arrows) appearing anechoic

cicular pattern of alternating hypoechoic nerve fascicles with hyperechoic epineurium. In the transverse plane, the cross-sectional view of hypoechoic fascicles surrounded by hyperechoic epineurium generates a honeycomb appearance. Figure 4.1 shows the echogenicity and echotexture of different anatomic structures in the transverse view.

Proper visualization of various anatomic structures on US requires the ultrasound beam to encounter the structure perpendicular to the surface of the tissue. If the ultrasound wave encounters the structure at a non-perpendicular angle, the beam is subsequently reflected off the structure obliquely and fails to be registered by the transducer, generating an artifactually dark, or hypoechoic, image (Fig. 4.2). This is termed *anisotropy* and is a common pitfall for inexperienced sonographers that can occur with as little as 2° – 3° deviation from a perpendicular angle [17]. It is important for clinicians to continuously manipulate the transducer during the examination, using tilting or heel-toeing maneuvers, to

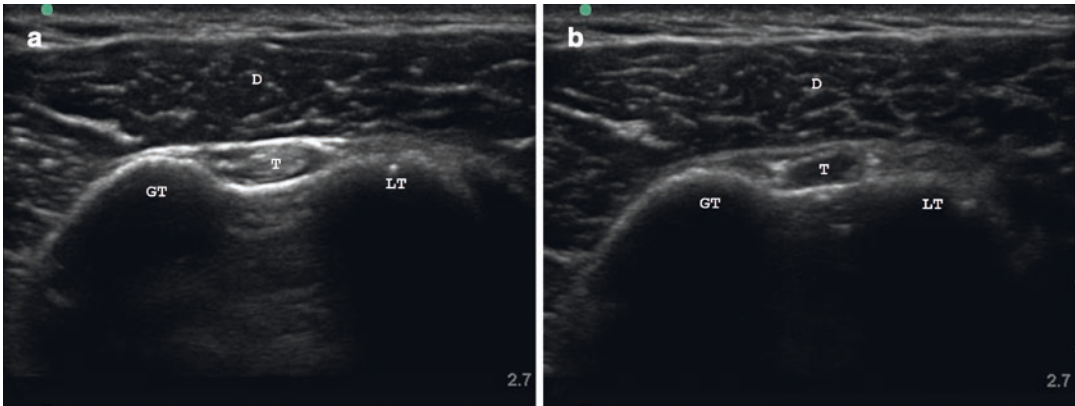


Fig. 4.2 Transverse view of the long head of biceps tendon in the bicipital groove demonstrating tendon anisotropy. (a) With the transducer oriented perpendicular to the tendon surface, the tendon (T) correctly appears as a hyperechoic fibrillar structure. (b) Tilting of the trans-

ducer generates an artifactually hypoechoic tendon image due to failure of the transducer to register the obliquely reflecting ultrasound waves. Deltoid muscle (D), greater tuberosity (GT), lesser tuberosity (LT)

direct the ultrasound beam perpendicular to surface of the target structure and generate an accurate image.

Sonographic Evaluation of the Biceps Brachii

Sonography of the biceps brachii involves systematic evaluation of the muscle and tendons in distinct anatomic zones as described by Brasseur [18], including the glenoid insertion of the LHB tendon, extension to the upper pole of the humeral head, the rotator interval, the bicipital groove, the upper and lower myotendinous junctions, the distal biceps tendon, and distal enthesis. It is imperative to understand the normal US appearance of the biceps brachii tendons and surrounding structures in order to properly recognize pathology.

Proximal Attachment at the Superior Glenoid

Assessment of the LHB tendon anchor at the superior glenoid is often restricted by the overlying acromion and clavicle, frequently limiting visualization of the labral-bicipital complex in this zone to anterior insertions. With the patient

seated upright and the shoulder placed in Middleton/Crass position of extension, slight internal rotation, and adduction, the transducer is applied to a small depression just inferior to the distal clavicle and medial to the anterior edge of the acromion [19]. This shoulder position can be accomplished by having the patient seated upright with the volar side of the hand placed on the ipsilateral buttock. In the transverse view, the labral-bicipital complex is visualized as an echogenic triangular structure adjacent to the upper glenoid composed of the LHB tendon overlying the superior labrum. In thin patients, posterior insertions of the LHB tendon may be visualized by placing the transducer just superior, or posterior, to the distal clavicle and medial to the acromion with the arm in a neutral position [19]. Dynamic examination of the biceps anchor and superior labrum has been described by bringing the arm through an arc of rotation in abduction and adduction while checking for labral displacement [20]. Injury to the superior labrum and/or LHB tendon anchor, including complete disruption, may be identified in this anatomic zone; however, it should be noted that visualization of the labral-bicipital complex on US is very challenging, especially in the setting of an intact rotator cuff and muscular body habitus, and is often impossible due to overlying osseous structures.

Therefore, magnetic resonance imaging (MRI) remains the gold standard for diagnosis of pathology in this region.

Upper Pole of Humeral Head

Evaluation of the LHB tendon continues along its intraarticular course as the tendon curves along the anterosuperior portion of the humeral head. With the shoulder in extension, slight internal rotation, and adduction, the transducer is placed perpendicular to the LHB tendon at the level of the humeral head cartilage [18]. The transverse view of the normal tendon should appear as an ovoid homogenous echogenic structure with a fibrillar pattern and comparable thickness to the contralateral shoulder. Intraarticular proximal biceps tendinopathy may be present on US examination of this anatomic region and is suggested by tendon thickening, decreased echogenicity, loss of the normal fibrillar pattern, and increased heterogeneity [18].

Rotator Interval

The shoulder is maintained in Middleton/Crass position of extension, internal rotation, and adduction to open the rotator interval and tighten the CHL. The transducer is shifted slightly lateral to visualize the LHB tendon within the rotator interval, remaining perpendicular to the biceps tendon [21]. Between the supraspinatus posterolaterally and subscapularis anteromedially, the echogenic components of the biceps pulley can be identified; the superficial CHL blends with the SGHL medially to form a U-shaped sling that resists medial displacement of the proximal biceps tendon (Fig. 4.3). Injury to the biceps pulley in this zone can lead to instability of the LHB tendon ranging from intermittent subluxation to frank dislocation of the tendon. Proximal biceps tendinopathy can also be identified in this anatomic zone, particularly in the setting of anterior supraspinatus tears and/or subacromial impingement syndrome [22].

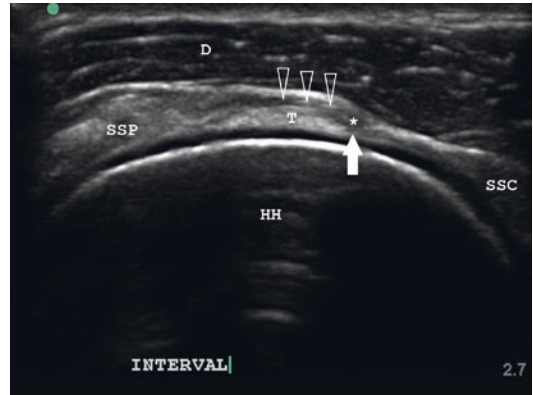


Fig. 4.3 Transverse view of the long head of biceps tendon in the rotator interval. The biceps tendon (T) is located between the supraspinatus (SSP) posterolaterally and subscapularis (SSC) anteromedially. The superficial coracohumeral ligament (arrowheads) can be seen blending medially with the superior glenohumeral ligament (arrows) to form the biceps pulley sling (asterisk) that stabilizes the tendon in the rotator interval. Deltoid muscle (D), humeral head (HH)

Bicipital Groove

Examination of the LHB tendon in the bicipital groove is performed with the shoulder in a neutral position, the elbow flexed to 90°, and the dorsum of the hand resting on the thigh. At the upper bicipital groove, a transverse scan of a normal LHB tendon reveals a round, uniformly echogenic structure centrally located in the osseous groove with fibers of the subscapularis and its aponeurosis coursing superficially. The proper position of the biceps tendon within the bicipital groove can be confirmed by identifying a hypoechoic area between the biceps tendon and the medial wall of the groove, termed the *triangle sign* (Fig. 4.4) [18]. The stability of the proximal biceps tendon can be dynamically evaluated by having the patient externally rotate the shoulder while maintaining visualization of the tendon in the bicipital groove in the transverse plane. A normal LHB tendon should remain centrally located within the groove as the patient rotates at the shoulder. The biceps tendon is normally surrounded by a small amount of fluid within the synovial pouch. Less than 1 mm of fluid is

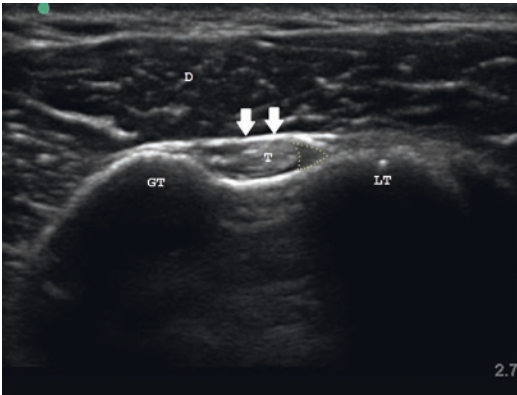


Fig. 4.4 Transverse view of the long head of biceps tendon centrally located in the groove. Presence of the hypoechoic triangle (yellow dotted line) between the biceps tendon (T) and medial wall of the groove confirms normal tendon position and static stability. Deltoid muscle (D), greater tuberosity (GT), lesser tuberosity (LT), transverse humeral ligament (THL)

thought to be physiologic, while greater than 3 mm of fluid is deemed a pathologic peritendinous effusion [23]. The entire length of the bicipital groove should be scanned, as fluid and debris surrounding the biceps tendon can pool distally in the dependent area of the sheath with the patient seated upright. Pertinent pathology in this anatomic region includes proximal biceps instability arising from biceps pulley injury and/or subscapularis tear, biceps tendinopathy or tenosynovitis, and complete rupture of the LHB tendon with an empty groove seen on ultrasound.

Distal Attachment at the Radial Tuberosity

Visualization of the distal biceps tendon is best performed in the transverse view using an anterior approach with the elbow in full extension and the forearm in forced supination. The transducer is placed at the mid-arm and moved distally until the transition to the distal biceps tendon and the lacertus fibrosis is seen. The distal biceps tendon is located superficial to the brachialis muscle and lateral to the brachial artery, which can be used as an additional landmark to locate the tendon (Fig. 4.5). The transducer is then moved distally

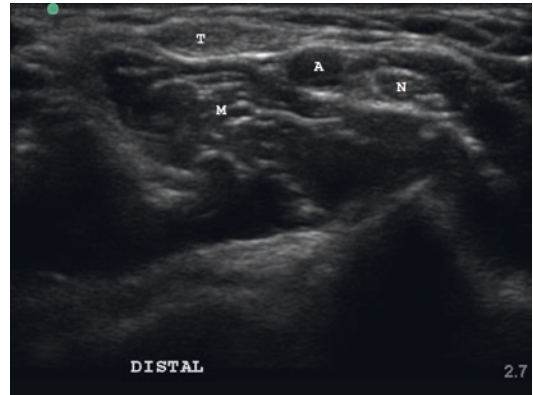


Fig. 4.5 Transverse view of the distal biceps tendon (T) in the antecubital fossa located superficial to the brachialis muscle (M) and lateral to the brachial artery (A) and median nerve (N)

to follow the distal biceps tendon down to its attachment on the radial tuberosity in both transverse and longitudinal planes. If full elbow extension is restricted due to pain or stiffness, or if tendon anisotropy limits tendon visualization from the anterior approach, other approaches may be used to image the distal biceps tendon. The posterior approach is performed with the elbow in 90° of flexion and maximum pronation (cobra position); while this approach provided excellent transverse and longitudinal views of the distal biceps enthesis, dynamic examination of the tendon through an arc of pronation-supination is not possible in this position [24].

Dynamic evaluation of the distal biceps tendon in the longitudinal view can be accomplished using either a lateral or medial approach. The lateral approach is performed with the elbow flexed to 90° and fully supinated. The transducer is placed parallel to the distal biceps tendon and over the lateral aspect of the forearm extensor musculature [25]. While this approach minimizes tendon anisotropy due to optimal parallel arrangement between the tendon and the transducer, evaluation of the distal insertion may be limited by the overlying supinator muscle and the trajectory of the tendon insertion at tuberosity. The insertion of the distal biceps tendon tends to remain oriented in an ulnar direction, even in maximum supination, which restricts visualiza-

tion from the lateral elbow. The medial approach through the flexor-pronator acoustic window was described by Smith et al. [26] and provides better visualization of the ulnarly direct tendon insertion than the lateral view while maintaining minimal tendon anisotropy through a similar parallel approach. With the elbow in 90° of flexion and full supination, the transducer is placed just proximal to the medial epicondyle and parallel to the humeral shaft. The transducer is then translated anteriorly until the distal biceps tendon is identified and then followed distally to its insertion at the tuberosity.

Diagnostic Sonography for Biceps Pathology

Proximal Biceps Anchor Lesions

Lesions involving the superior labrum and proximal biceps anchor are a well-recognized cause of shoulder pain. Various mechanisms of injury have been described including microtraumatic damage in the setting of repetitive overhead throwing activities and single traumatic events such as a forceful traction load or direct compression load to the arm [27]. The pathology tends to originate at the posterior aspect of the superior labrum and extend anteriorly, hence the name Superior Labrum Anterior to Posterior (SLAP) tear [27]. Originally, four types of SLAP tears were described by Snyder et al. [28]; this classification has expanded over the years to include six additional variants of SLAP lesions. Of the ten types of SLAP tears currently described, seven include either discrete tears of the biceps tendon (types IV and X) or stripping of the proximal biceps insertion off the superior labrum or glenoid attachment (types II, V, VI, VII, and IX) [29]. However, precise classification of SLAP tear morphology on imaging, even magnetic resonance arthrography, remains challenging. Literature regarding the use of US for the diagnosis of superior labrum tears and insertional lesions of the LHB tendon is quite sparse. Currently, there is no published data on the sensitivity, specificity, or accuracy of this imaging

modality for the detection of SLAP tears and biceps anchor lesions.

Proximal Biceps Instability

Stability of the LHB tendon depends predominantly on the soft tissue restraints that make up the biceps pulley system – the SGHL, CHL, subscapularis tendon, and supraspinatus tendon. Osseous morphology of the bicipital groove has also been shown to contribute to tendon stability, though to a lesser extent [30]. Proximal biceps tendon instability almost always presents in combination with other inflammatory, degenerative, or traumatic shoulder pathology. The pathology may be primary, leading to secondary failure of the pulley system and LHB tendon instability. Subacromial impingement, rotator cuff tendinitis, and glenohumeral arthritis can all lead to biceps tenosynovitis and/or long-standing biceps tendinosis with gradual attenuation of the biceps pulley system. Traumatic injury to the biceps anchor at the superior labrum and rotator cuff tendons can also lead to proximal biceps tendon instability. Rotator cuff tears, particularly involving the subscapularis tendon, are the most common associated pathology. This is thought to be related to lost protection of biceps tendon from the coracoacromial arch with subsequent tendon impingement and attritional damage [31]. Conversely, associated shoulder pathology may arise secondary to biceps pulley injury. Primary instability of the LHB tendon can cause repetitive frictional injury to an intact supraspinatus or subscapularis with resultant partial tearing [32].

While the exact sequence of events varies greatly depending on the underlying pathology, ultimately proximal biceps tendon instability involves damage to one or more of the four components of the biceps pulley system. Several classification systems have been developed, which categorize the pulley lesions based on a variety of variables, including the injured structure(s), location of instability, and direction of the tendon dislocation or subluxation [32–34]. The Bennett classification is most commonly used and subdivides biceps pulley lesions into five types [33].

Type I is an isolated articular-sided subscapularis injury. Type II is an isolated injury to the SGHL-CHL complex involving the medial band of the CHL (mCHL). Type I and II injuries are characterized by medial tendon subluxation but not frank dislocation. Type III is an injury to the subscapularis and SGHL-mCHL complex with resultant medial intraarticular dislocation of the tendon deep to the subscapularis. Type IV is an injury to the lateral band of the CHL that allows the tendon to dislocate medially superficial, or anterior, to the subscapularis due to loss of tension on the entire medial sling. Type IV injuries have a high association with supraspinatus tears. Type V is an injury to all four structures of the biceps pulley system and presents with medial dislocation typically deep to the subscapularis.

Sonography is a highly accurate imaging modality for the detection and characterization of LHB tendon instability [35, 36]. In addition to visualizing the static position of the tendon and identifying injured structure(s), ultrasound also permits dynamic evaluation of the instability pattern. With the arm resting at the patient's side, the elbow flexed to 90°, and the dorsum of the hand placed on the thigh, the transducer is applied to the proximal bicipital groove and translated superiorly to visualize the rotator interval. Injury to structures of the biceps reflective pulley can be identified as discontinuity of the U-shaped sling normally visualized at this level. Degree of instability, including subluxation versus dislocation

and dynamic versus static, depends on the extent of injury to the soft tissue stabilizers. Dynamic stability of the LHB tendon is assessed by externally rotating the patient's arm while maintaining the elbow tight to the patient's side [37]. Subluxation is characterized by absence of the normal triangle sign, defined as loss of the distinct border between the biceps tendon and the groove as the tendon perches on the medial edge [18]. Dislocation of LHB tendon can occur superficial or deep to the subscapularis; superficial tendon dislocation anterior to the subscapularis suggests a lateral CHL lesion with an intact subscapularis (Fig. 4.6a), while intraarticular tendon dislocation deep to the subscapularis signifies a concomitant subscapularis tear (Fig. 4.6b) [33]. Sonography has demonstrated a sensitivity of 96%, specificity of 100%, and an accuracy of 100% for the diagnosis of LHB tendon subluxation or dislocation [35, 36].

Proximal Biceps Tendinopathy

Tendinopathy of the proximal biceps tendon encompasses a spectrum of pathology including tendon inflammation (*tendinitis* or *tenosynovitis*) and tendon degeneration (*tendinosis*) advancing from intrasubstance deterioration to partial tendon tearing and ultimately to complete rupture of the LHB tendon. Similar to other proximal biceps pathology, tendinopathy of the LHB tendon fre-

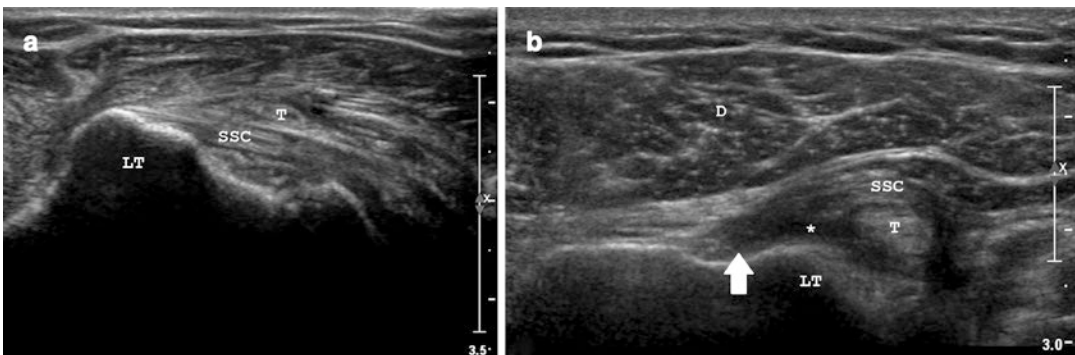


Fig. 4.6 Instability of the long head of biceps tendon on sonography. (a) Transverse view of the long head of biceps tendon (T) dislocated out of the groove and lying superficial to an intact subscapularis (SSC). (b) Transverse

view of a dislocated long head of biceps tendon (T) lying deep to the subscapularis (SSC) with an empty groove (arrow). There is a concomitant subscapularis tear (asterisk). Deltoid muscle (D), lesser tuberosity (LT)

quently occurs in association with other shoulder conditions, ranging from impingement, bursitis, rotator cuff disorders, glenohumeral osteoarthritis, superior labral tears, and acromioclavicular joint pathology [38]. Mechanical impingement of the LHB tendon beneath the coracoacromial (CA) arch is a common cause of progressive LHB tendinopathy, particularly in patients with rotator cuff pathology and/or impingement syndrome (acromial bone spur or thickening of the CA ligament) [39]. Isolated primary LHB tendinopathy is rare, occurring in only 5% of patients with proximal biceps pathology [40]. Acute proximal biceps tendinitis, characterized by tendon hyperemia and swelling, typically arises from mechanical irritation of the tendon precipitated by repetitive overhead activities. If the mechanical microtrauma persists, acute tenosynovitis can evolve to chronic tendinosis, with less inflammatory reaction and more advanced tendon degeneration and scarring. Microscopic tendon degradation with collagen breakdown and fibrinoid necrosis can progress to macroscopic delamination and ultimately to complete tendon rupture. Spontaneous LHB rupture most often occurs at the proximal biceps anchor and proximal myotendinous junction.

Ultrasound evaluation of the LHB tendon should begin with visualization of the intraarticular portion at the superior pole of the humeral head. The shoulder is placed in extension, and the transducer is applied in a transverse view of the LHB tendon at the level of the humeral head cartilage. At this level, tendon thickening suggests LHB tendinopathy. Focal hypertrophy of the intraarticular LHB tendon can also lead to tendon entrapment, mechanical locking of the shoulder, and restricted range of motion. Termed the *hourglass biceps*, the thickened intraarticular tendon engages the superior aspect of the bicipital groove with shoulder elevation, preventing normal tendon excursion into the groove and leading to a 10°–20° loss of passive glenohumeral elevation and abduction with preserved rotation [41]. In addition to static measurements of tendon thickness, dynamic US of the intraarticular LHB tendon can help identify hourglass biceps pathol-

ogy and dynamic entrapment. The transducer is rotated to a longitudinal view of the LHB tendon at the upper pole of the humeral head, and tendon diameter is measured. The arm is then maximally abducted in the scapular plane, and LHB tendon diameter is measured at the same level. A 10% increase in tendon thickness or visible tendon buckling is considered diagnostic of an hourglass biceps deformity. This dynamic ultrasound test demonstrated a sensitivity of only 50% but a specificity of 100% [42].

Sonographic examination continues with evaluation of the LHB tendon in the bicipital groove. The shoulder is in a neutral position with the elbow flexed to 90° and the dorsum of the hand resting on the thigh. A transverse scan of the LHB tendon and sheath begins at the entrance to the bicipital groove and moves distally. The amount of fluid in the tendon sheath can be measured on both transverse and longitudinal views (Fig. 4.7). LHB tendinosis is most strongly associated with a moderate peritendinous effusion measuring 2–3 mm, while acute tenosynovitis can be associated with a much larger effusion [23]. Color Doppler mode may reveal focal hypervascularity of the tendon sheath consistent with acute tenosynovitis (Fig. 4.7c, d). Features of LHB tendinopathy on ultrasound include a rounded and thickened tendon appearance, irregular tendon borders, increased tendon heterogeneity, and focal hypoechoic fissures (Fig. 4.7). Complete rupture of the LHB tendon is characterized by absence of the LHB tendon within the groove and visualization of the thickened retracted tendon distally in the arm. Ultrasound has a reported sensitivity of 75%, specificity of 100%, and accuracy of 98% for diagnosis of complete LHB ruptures [36]. Similarly, ultrasound diagnosis of full-thickness LHB tendon tears has shown a sensitivity of 88–100%, specificity of 97–98%, and accuracy of 97–98% [36, 43]. However, for diagnosis of partial-thickness LHB tendon tears, ultrasound has a poor sensitivity ranging from 27% to 46% and accuracy of 81–88% when compared to surgical findings [36, 43]. Therefore, while US is highly accurate for the diagnosis of complete LHB rupture and full-

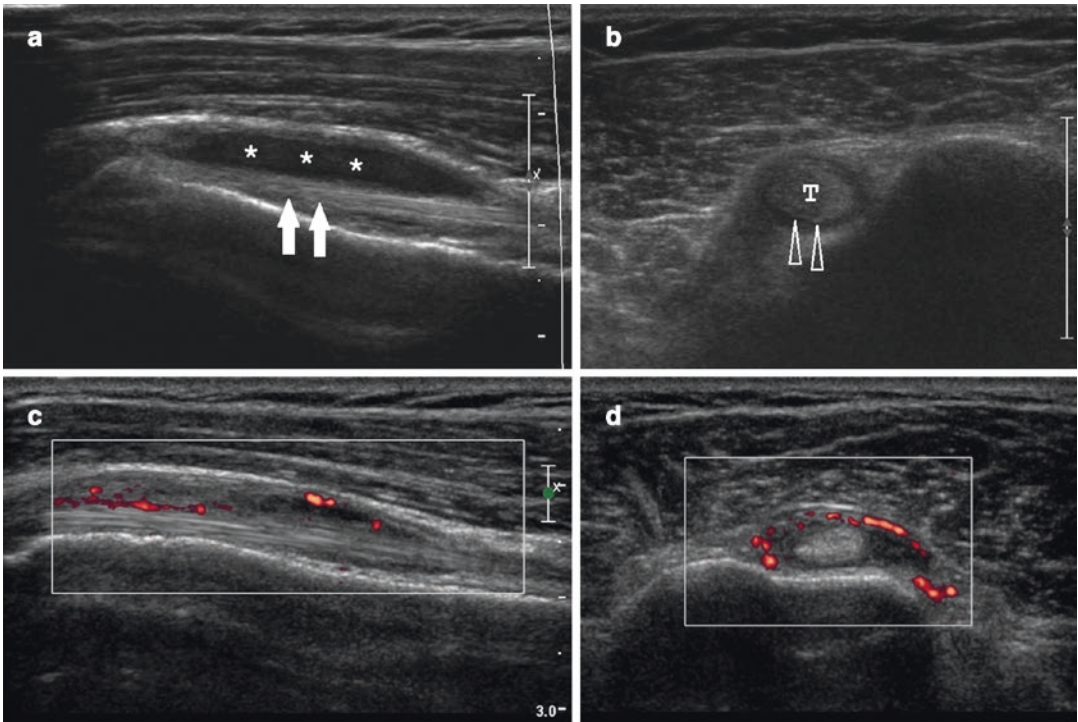


Fig. 4.7 Long head of biceps tendonopathy on sonography. Longitudinal (a) and transverse (b) views of the long head of biceps tendon (T) in the groove show increased peritendinous fluid (asterisks), irregular tendon borders (arrowheads), and increased tendon heterogeneity with

focal hypoechoic fissures (arrows). Color Doppler mode in the longitudinal (c) and transverse (d) views show hyperemia of the tendon sheath (red) consistent with tenosynovitis

thickness tears of the LHB tendon, it is far less reliable for detection of LHB tendonopathy and partial tears.

Distal Biceps Tendinopathy

Distal biceps tendon pathology includes a wide range of disease spanning from tendinosis and partial tearing to complete tendon rupture. Tears of the distal biceps tendon are far less common than those involving the LHB tendon and comprise less than 10% of all biceps brachii injuries [44]. Partial tears typically occur in a hypovascular zone located 1–2 cm proximal to the radial tuberosity. At this level, the distal biceps tendon is supplied by a thin longitudinal plexus of vessels with variable arterial contributions. Lack of vascularity in this area hinders the normal tendon

repair mechanisms and leads to intrasubstance degeneration [45]. Mechanical impingement of the distal biceps tendon during forearm rotation also contributes to progressive tendon damage, as the tendon is repeatedly drawn between the radius and ulna with pronation. Recurrent traction forces on the radial tuberosity can lead to osseous hypertrophy and formation of an enthesophyte, which can further impinge on the distal biceps tendon with forearm rotation [46].

Ultrasound imaging of distal biceps tendon pathology is first performed from an anterior approach with the elbow in full extension and forearm in maximum supination. Visualization of the distal-most tendon and insertion at the radial tuberosity is performed via a posterior approach with the elbow in the cobra position of 90° elbow flexion and maximum pronation. Distal biceps tendonopathy is characterized by diffuse heterog-

enous thickening of the tendon, focal areas of hypoechogenicity and fissures, and loss of the normal fibrillar pattern indicating focal disruption of tendon fibers (Fig. 4.8). On the longitudinal view, fissuring is better visualized with the elbow in slight flexion to relax the tendon and avoid collapse of the fissures [18]. In cases of chronic tendinosis, tiny foci of calcification may be seen as small hyperechoic spiculated fragments (Fig. 4.8b). The bicipitoradial bursa, usually invisible on US and MRI, may become dilated with fluid and be visible as an anechoic

mass deep to the distal biceps tendon (Fig. 4.8c). An enthesophyte may be identified at the radial tuberosity and may be seen contacting the tendon in maximum pronation.

Distal Biceps Tendon Rupture

Complete ruptures of the distal biceps tendon typically arise from a single traumatic event in which an excessive eccentric load forces a flexed elbow into extension [47]. This mechanism often

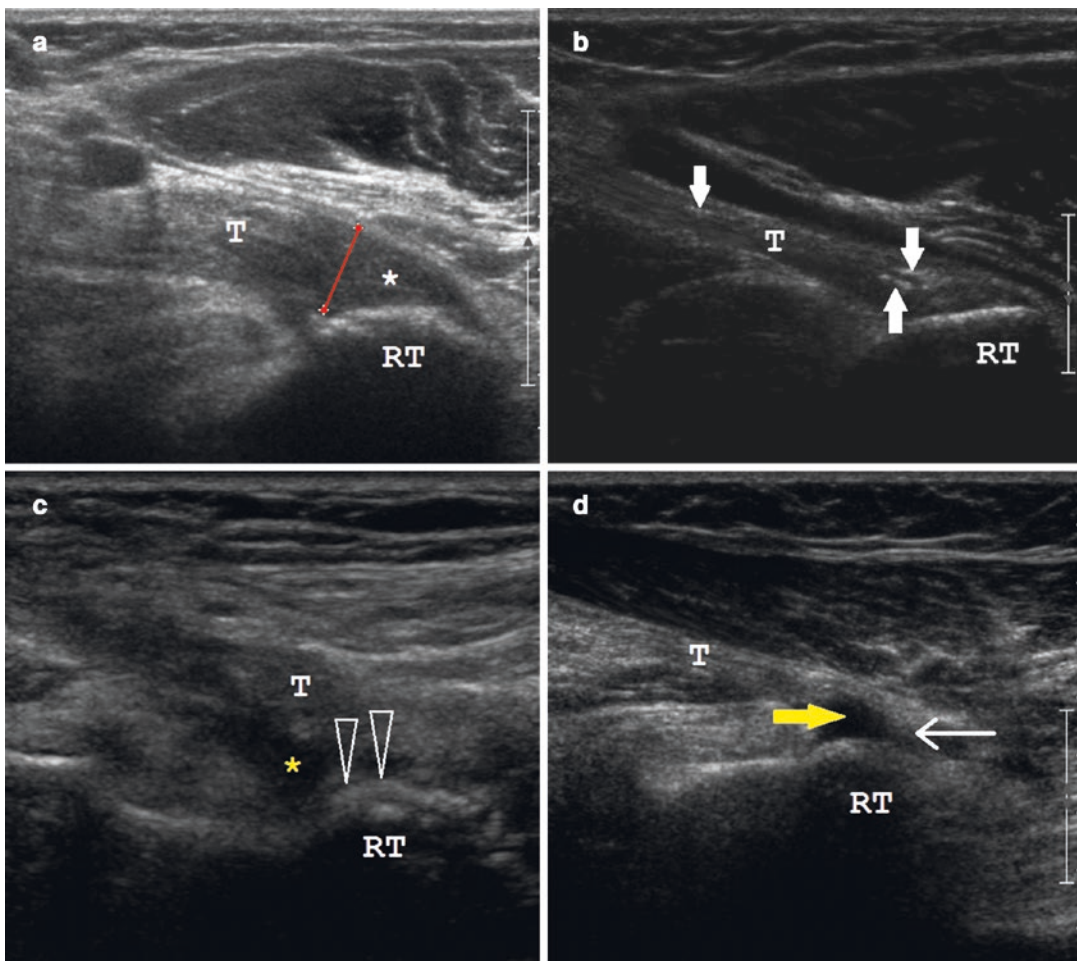


Fig. 4.8 Distal biceps tendinopathy on sonography. (a) Longitudinal view of the distal biceps tendon (T) shows tendon thickening (red line) and increased tendon heterogeneity with hypoechoic areas and loss of the normal fibrillar pattern (white asterisk) suggesting disruption of tendon fibers. (b) Longitudinal view of the distal biceps tendon reveals small hyperechoic calcium deposits within

the tendon (thick white arrows). (c) Longitudinal view of the distal biceps tendon shows fluid within the bicipitoradial bursa (yellow asterisk) and an enthesophyte (arrowheads) at the radial tuberosity (RT). (d) Longitudinal view of the distal biceps enthesis shows a partial tear (yellow arrow) with some fibers remaining in continuity (thin white arrow)

leads to an avulsion of the distal biceps tendon from the radial tuberosity [48]. A complete tear is often clinically evident, with antecubital ecchymosis, irregular biceps brachii contour secondary to proximal retraction of the muscle belly, and an abnormal hook test. First described by O’Driscoll et al. [49], the hook test is performed with the elbow in 90° of flexion as the examiner attempts to hook the lateral aspect of the distal biceps tendon with his or her index finger while the patient supinates against resistance. A positive test is defined as absence of the cord-like distal biceps tendon and has demonstrated 100% sensitivity and specificity for the detection of distal biceps tendon tears [49]. The extent of retraction depends on the continuity of the lacertus fibrosus. If a well-developed lacertus fibrosus remains intact, a complete distal biceps tendon rupture may exhibit minimal tendon retraction. Additionally, an intact lacertus fibrosus may be difficult to distinguish from an intact distal biceps tendon on hook test examination. Advanced imaging with US and MRI can be helpful in equivocal cases to confirm diagnosis of a complete tendon rupture and provide additional information about the integrity of the lacertus fibrosus, level of tendon rupture, extent of proximal retraction, and quality of the torn tendon.

Sonographic evaluation for a suspected distal biceps rupture begins with longitudinal and transverse views of the distal biceps tendon from an anterior approach with the elbow in extension (or slight flexion if limited by pain) and forearm in supination. Ultrasound findings of an acute complete distal biceps tendon rupture include tendon discontinuity, snake-like pattern of the detensioned tendon on longitudinal view, peritendinous effusion, and a fluid-filled gap generated by proximal tendon retraction. The tendon stump can be identified as a hypertrophic, hyperechoic mass with posterior acoustic shadowing secondary to refraction artifact (Fig. 4.9). In addition to the diagnosis of a complete distal biceps tendon rupture, US can also be utilized to measure the degree of proximal tendon retraction. The extended field-of-view (FOV) scanning technique generates panoramic longitudinal images that permit the measurement of structure length and the distance between two anatomic structures. Greater than 8 cm of distal biceps tendon retraction correlates with a torn lacertus fibrosus [50].

Ultrasound has been shown to be an exceptionally accurate imaging modality for the diagnosis of complete distal biceps tendon ruptures with reported sensitivity ranging 95–98% com-

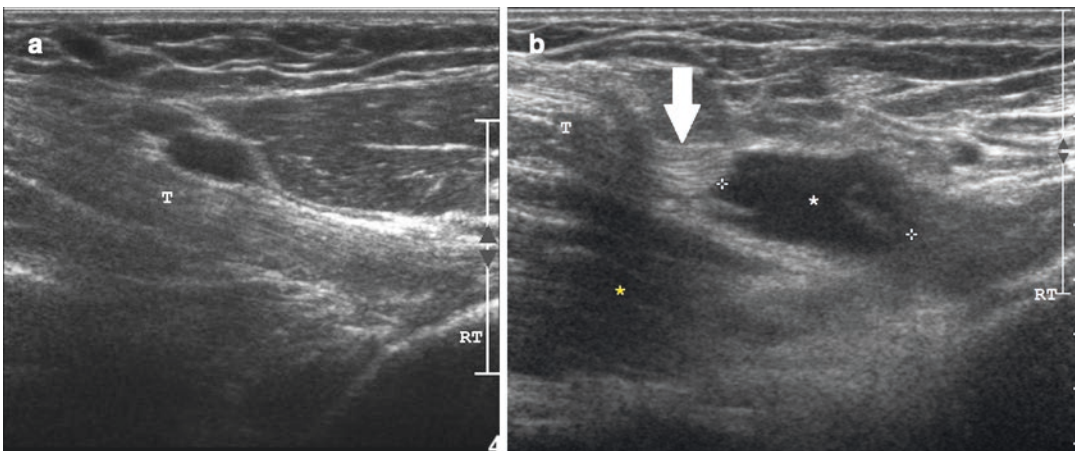


Fig. 4.9 Distal biceps rupture on sonography. (a) Longitudinal view of a normal distal biceps tendon (T) insertion at the radial tuberosity (RT). (b) Longitudinal view shows complete distal biceps tendon discontinuity

with a fluid-filled space (white asterisk), proximal retraction of the hyperechoic tendon stump (arrow) with detensioned fibers, and posterior acoustic shadowing (yellow asterisk) secondary to refraction artifact

parable to 96% sensitivity with MR imaging [51]. Iobo et al. [52] investigated the accuracy of ultrasound for distinguishing a complete distal biceps tendon rupture from a partial tendon tear or a normal biceps tendon. Sonography demonstrated 95% sensitivity, 71% specificity, and 91% accuracy for the diagnosis of complete versus partial distal biceps tendon tears. In particular, detection of posterior acoustic shadowing on US demonstrated a sensitivity of 97%, specificity of 100%, and accuracy of 98% for distinguishing a complete distal biceps tendon rupture from a normal tendon. While the presence of posterior shadowing highly correlates with complete tendon rupture, it is significantly less sensitive (43%) for differentiating a partial distal biceps tear from a normal tendon [52].

Ultrasound-Guided Treatments for Biceps Pathology

Ultrasound guidance for interventional musculoskeletal procedures provides visualization of adjacent anatomic structures to guide accurate instrument placement and minimize risk of iatrogenic injury. Numerous therapies have been described for the treatment of tendinous pathology, including peritendinous corticosteroid and local anesthetic injections, intratendinous injections of regenerative agents (i.e., platelet-rich plasma (PRP), autologous whole blood, bone marrow-derived stem cells, autologous tenocytes, and amniotic stem cells), prolotherapy, hydrodissection, tendon scraping, percutaneous needle fenestration and tenotomy, and minimally invasive tendon debridement using ultrasonic energy [53]. These procedures can be performed using an in-plane or out-of-plane technique. With the *in-plane* approach, the long axis of the needle is aligned parallel to the long axis of the transducer and traverses the plane of the ultrasound. This technique allows visualization of the entire length of the needle including the tip and is the most accurate approach. The *out-of-plane* technique is performed with the needle aligned perpendicular to the long axis of the transducer. The needle tip enters the skin out of the plane of the ultrasound

and aims to enter the plane, generating a transverse axis image of the needle. This approach is more challenging, as it is difficult to distinguish the needle tip from the needle shaft using a transverse axis view.

Long Head of Biceps Peritendinous Injection

Injections of corticosteroid and/or local anesthetic agents around the LHB tendon can be performed in the rotator interval or the biceps tendon sheath within the groove. While the majority of LHB tendon injections are done at the level of the bicipital groove, injections to the rotator interval allow more injectate to flow back into the glenohumeral joint, rendering this technique ideal for intraarticular biceps tendinopathy and concomitant glenohumeral pathology such as adhesive capsulitis and osteoarthritis [54]. The LHB tendon in the rotator interval is visualized in the transverse plane with the shoulder in the Middleton/Crass position of extension, internal rotation, and adduction by having the patient rest the volar aspect of the hand on the ipsilateral buttock. The LHB tendon may first be identified in the bicipital groove and then followed cranially until interposed between the supraspinatus posteriorly and subscapularis anteriorly. Once visualized, the needle is then introduced from lateral to medial using an in-plane approach, aiming for the space between the CHL superficially and the tendon lying beneath [55].

An ultrasound-guided injection to the LHB tendon sheath in the bicipital groove is performed with the shoulder in a neutral position, the elbow flexed to 90°, and the dorsum of the hand resting on the thigh. Slight external rotation of the arm allows the bicipital groove to face more anterolaterally and can improve visualization. Needle guidance may be achieved using a transverse or longitudinal view of the tendon. In the transverse view, the transducer is positioned lateral to the coracoid and perpendicular to the LHB tendon. The THL can be readily identified as a hyperechoic structure superficial to the tendon. Color Doppler mode can be used to identify the ascend-

ing branch of the anterior circumflex humeral artery at the lateral aspect of the bicipital groove and avoid puncturing it during the injection [56]. The target area should be positioned in the lateral one-third of the screen to decrease the needle trajectory through the deltoid muscle. The needle is then introduced from lateral to medial using an in-plane approach at an oblique angle of 30°–45° aiming for the space between the LHB tendon and the THL, taking care to avoid tendon penetration. As the drug is delivered to the bicipital sheath, fluid can be seen surrounding the tendon (Fig. 4.10) [54]. Conversely, an injection to the longitudinal axis of the tendon can be performed by rotating the transducer parallel to the tendon. The needle is then inserted in plane from caudal to cranial aiming just superficial to the LHB tendon to avoid injecting the subdeltoid bursa instead [57].

Shoulder girdle injections, including those to the LHB tendon sheath, have traditionally been performed using palpation of anatomical landmarks to guide needle placement. Yet, even experienced clinicians are unable to palpate the bicipital groove with a great degree of accuracy and consistently localize the groove medial to its actual location [58]. The use of ultrasound guid-

ance has been shown to improve the accuracy and efficacy of injections targeting the LHB tendon. Hashiuchi et al. [59] evaluated 30 patients with LHB tenosynovitis and/or tendinitis who were randomly assigned to ultrasound-guided or landmark-guided corticosteroid injections to the biceps tendon sheath with a contrast agent followed by computed tomography (CT) imaging to confirm injection location. Accurate placement into the tendon sheath was noted in 13 of 15 US-guided injections (86.7%) compared to only 4 of 15 landmark-guided injections (26.7%; $p < 0.05$). Zhang et al. [60] performed a prospective comparative study of 98 patients with symptomatic LHB tendinopathy who were randomized to ultrasound-guided or landmark-guided corticosteroid injections. Patients who received an ultrasound-guided injection demonstrated significantly greater reduction in pain ($p < 0.05$) and greater improvement in function ($p < 0.01$) compared to patients with landmark-guided injections at a mean follow-up of 34 weeks. There were no reported adverse events in either group. Another randomized prospective study comparing ultrasound-guided to landmark-guided corticosteroid injections for LHB tendinopathy found that ultrasound-guided injections resulted in

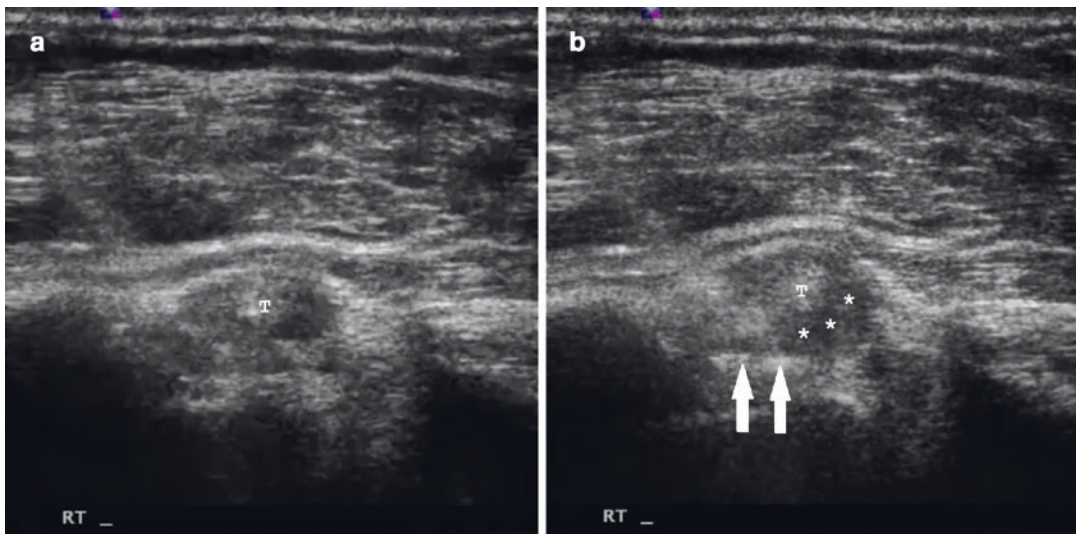


Fig. 4.10 Ultrasound-guided injection to the long head of biceps tendon sheath. Transverse views of the long head of biceps tendon (T) in the groove before (a) and after (b) injection. The needle (arrows) is directed using

an in-plane approach from lateral to medial. Increased fluid is seen surrounding the tendon after the injection (asterisks)

superior clinical improvement, as measured by VAS, SANE, and QuickDASH scores, at 4 weeks and 6 months ($p < 0.05$). Ultrasound-guided injections were also faster and produced less patient discomfort during the procedure [61]. Compared to fluoroscopy-guided biceps tendon sheath injections, ultrasound-guided injections demonstrate a first attempt success rate of 90.6% compared to 74% for fluoroscopy ($p < 0.05$). There was no significant difference in the final attempt success rate and visual analog scale score between the two groups [62].

Long Head of Biceps Percutaneous Tenotomy

Operative treatment options for LHB tendon disorders primarily include debridement, tenotomy, and tenodesis. Compared to tenodesis, arthroscopic LHB tenotomy is a quick and technically simple procedure with low surgical morbidity, less intensive postoperative rehabilitation required, and equivalent patient satisfaction and clinical outcomes [63]. Ultrasound-guided percutaneous LHB tenotomy has the added benefit of being a less invasive procedure that can be performed without the risks and costs associated with general anesthesia.

At the present time, there is one case report detailing the first ultrasound-guided LHB tenotomy performed under local anesthesia on a 59-year-old male with a very good functional result [64]. The patient is positioned supine with the arm in a neutral position, prepped and draped in typical sterile fashion. A transverse scan of the LHB tendon in the groove is obtained with a sterile transducer 1 cm proximal to the superior border of the pectoralis major tendon and inferior to the THL. Local anesthetic is injected to the overlying skin and subcutaneous tissue and then advanced in plane to anesthetize the LHB tendon and sheath at this level. A 0.5 cm incision is made superficially along the needle track, and an arthroscopic hook blade is percutaneously introduced from lateral to medial using an in-plane approach to enter the biceps sheath. The hook knife is placed between the LHB tendon and the

bone, and appropriate position is confirmed on ultrasound. The sharp end of the hook blade is then pulled through the tendon from deep to superficial until resistance is no longer felt. Complete tenotomy is confirmed by noting a fluid gap between the severed tendon ends. The primary downside to this approach described by Greditzer et al. [64] is the distal location of the tenotomy, leaving a very long proximal stump that could lead to residual pain or intraarticular mechanical obstruction as well as a short distal stump that may cause a problem if the procedure needs to be revised to an open tenodesis for cramping or cosmetic deformity.

Intraarticular LHB tenotomy using ultrasound guidance has been only described in feasibility cadaveric studies to date [65, 66]. Aly et al. [65] found that use of an arthroscopic hook blade introduced intraarticularly through an anterior portal and cutting the tendon from deep to superficial results in complete tendon transection without iatrogenic injury to the humeral head cartilage or rotator cuff tendons. Atlan et al. [66] reported intraarticular LHB tenotomy using a backward cutter through a single portal, either anterior or posterior. The authors also described the *groove alone test* to ensure no soft tissue was entrapped between the cutting instrument and the LHB tendon prior to tenotomy, to minimize risk of iatrogenic injury. After placement of the backward cutter between the superior aspect of the LHB tendon and the articular surface of the supraspinatus, the LHB tendon is mobilized with the instrument while scanning the length of the tendon from the rotator interval to the distal end of the bicipital groove. If no other tissue is caught by the cutter, mobilization of the intraarticular LHB tendon creates a movement of the entire tendon, while no other anatomic structures move (“groove alone”). Failure of the LHB tendon to move when the instrument mobilized the intraarticular LHB tendon suggests entrapment of soft tissue between the cutter and the tendon and indicates that it is not safe to perform the tenotomy [66]. Larger studies and prospective clinical investigations are needed to confirm the reliability of these techniques and determine functional outcomes compared to arthroscopic tenotomy.

Distal Biceps Tendon Injection

Both peritendinous and intratendinous injections have been described for the treatment of distal biceps tendinopathy. Peritendinous corticosteroid injections have been used in the treatment of partial tears or tendinosis of the distal biceps tendon to reduce pain and facilitate rehabilitation. Though satisfactory outcomes have been reported, the use of peritendinous corticosteroid injections carries the potential risk of tendon rupture [67]. Additionally, histologic studies of chronic tendinopathy suggests no significant inflammatory role by 4 months, questioning the utility of anti-inflammatory agents in the treatment of this condition [68]. As our understanding of distal biceps tendinopathy has advanced, there has been growing interest in the role of intratendinous injections of various regenerative agents, typically platelet-rich plasma (PRP), and tendon fenestration to stimulate a healing response.

Numerous ultrasound-guided peritendinous and intratendinous injection approaches have been described in cadaveric studies. Sellon et al. [69] performed a cadaveric study with injectable latex to evaluate the accuracy of four peritendinous approaches and three intratendinous approaches using both anterior and posterior

windows. All 18 peritendinous injections were successful, but 1 anterior approach injection had penetration of the brachial artery. While the posterior approach decreased the risk of vascular injury, it also demonstrated limited proximal peritendinous spread and injectate placement within the supinator muscle in proximity to the posterior interosseous nerve. Intratendinous injections were successful in 14 of 15 (93%) cases with one anterior intratendinous approach placing injectate into the peritendinous space alone.

Selection of approach and viewing axis depends on the area being targeted and clinician preference. The posterior approach is usually favored to avoid neurovascular injury. The patient is supine with the extremity in the cobra position of 90° elbow flexion and maximum pronation. The transducer is applied to the dorsal forearm, and a longitudinal view of the distal biceps tendon is obtained. The needle is then introduced from radial to ulnar using an in-plane approach and advancing through the supinator to reach the distal biceps tendon and peritendinous space (Fig. 4.11). Using this approach, the injection can be delivered to three different locations: (1) superficial peritendinous space between the ulnar surface of the tendon and the deep fascia of the

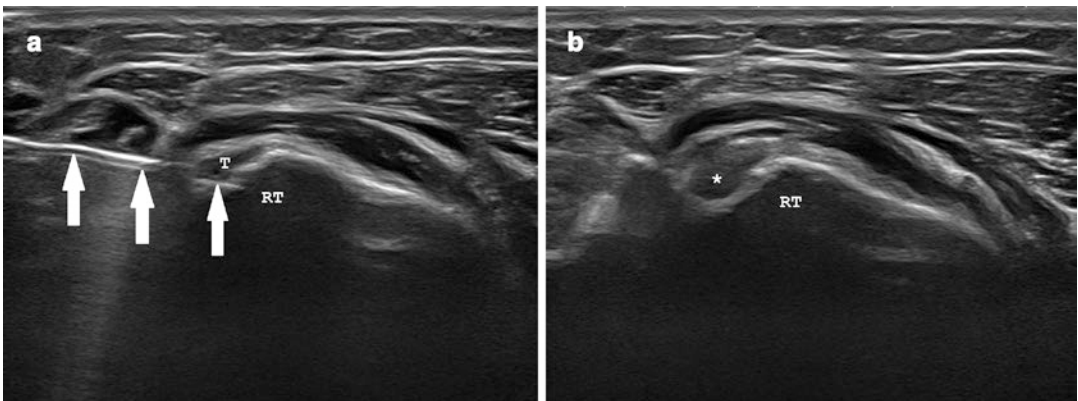


Fig. 4.11 Ultrasound-guided injection to the distal biceps tendon using a posterior approach. Longitudinal views of the distal biceps tendon (T) before (a) and after (b) platelet-rich plasma injection (PRP). The tendon appears hypoechoic, consistent with long-standing tendinosis. The needle (arrows) is directed using an in-plane

approach from radial to ulnar. Dry needling of the tendon and radial tuberosity (RT) is first performed to generate intrasubstance cleavage planes for maximum PRP penetration, followed by intratendinous delivery of the injectate (asterisk)

supinator in the region of the interosseous bursa, (2) intratendinous, or (3) deep peritendinous space between the radial surface of the tendon and radius by passing transtendinous to enter the bicipitoradial bursa.

Conclusion

Sonography is a relatively low-cost, portable imaging modality that enables dynamic real-time assessment of assorted musculoskeletal pathology. The use of ultrasound for the diagnosis of various proximal and distal biceps brachii injury, including tendinopathy, tendon instability, and complete rupture, has been well described. Sonography also permits immediate therapeutic interventions for a spectrum of biceps pathology, including guided peritendinous corticosteroid and local anesthetic injections, intratendinous injections of regenerative agents such as PRP, percutaneous needle fenestration, and tenotomy. A thorough understanding of the normal US appearance of the biceps brachii tendons and surrounding structures is necessary to properly identify and manage biceps pathology with US.

References

1. Stevens K, Kwak A, Poplawski S. The biceps muscle from shoulder to elbow. *Semin Musculoskelet Radiol*. 2012;16:296–315.
2. Smith J, Finnoff JT. Diagnostic and interventional musculoskeletal ultrasound: part 1. Fundamentals. *PM&R*. 2009;1:64–75.
3. Smith J, Finnoff JT. Diagnostic and interventional musculoskeletal ultrasound: part 2. Clinical applications. *PM&R*. 2009;1:162–77.
4. Nazarian LN. The top 10 reasons musculoskeletal sonography is an important complementary or alternative technique to MRI. *AJR Am J Roentgenol*. 2008;190:1621–6.
5. Finnoff JT, Hall MM, Adams E, Berkoff D, Concoff AL, Dexter W, Smith J. American Medical Society for Sports Medicine (AMSSM) position statement: interventional musculoskeletal ultrasound in sports medicine. *PM&R*. 2015;7:151–68.
6. Tuoheti Y, Itoi E, Yamamoto N, Seki N, Abe H, Minagawa H, Okada K, Shimada Y. Contact area, contact pressure, and pressure patterns of the tendon-bone interface after rotator cuff repair. *Am J Sports Med*. 2005;33:1869–74.
7. Werner A, Mueller T, Boehm D, Gohlke F. The stabilizing sling for the long head of the biceps tendon in the rotator cuff interval: a histoanatomic study. *Am J Sports Med*. 2000;28:28–31.
8. Kwon YW, Hurd J, Keith Yeager B, Ishak C, Walker PS, Khan S, Bosco JA III, Jazrawi LM. Proximal biceps tendon: a biomechanical analysis of the stability at the bicipital groove. *Bull NYU Hosp Jt Dis*. 2009;67:337–40.
9. Kulshreshtha R, Singh R, Sinha J, Hall S. Anatomy of the distal biceps brachii tendon and its clinical relevance. *Clin Orthop Relat Res*. 2007;456:117–20.
10. Skaf AY, Boutin RD, Dantas RW, Hooper AW, Muhle C, Chou DS, Lektrakul N, Trudell DJ, Haghghi P, Resnick DL. Bicipitoradial bursitis: MR imaging findings in eight patients and anatomic data from contrast material opacification of bursae followed by routine radiography and MR imaging in cadavers. *Radiology*. 1999;212:111–6.
11. Dirim B, Brouha SS, Pretterklieber ML, Wolff KS, Frank A, Pathria MN, Chung CB. Terminal bifurcation of the biceps brachii muscle and tendon: anatomic considerations and clinical implications. *AJR Am J Roentgenol*. 2008;191:W248–55.
12. Ghalayini SR, Board TN, Srinivasan MS. Anatomic variations in the long head of biceps: contribution to shoulder dysfunction. *Arthroscopy*. 2007;23:1012–8.
13. Kim KC, Rhee KJ, Shin HD, Kim YM. Biceps long head tendon revisited: a case report of split tendon arising from single origin. *Arch Orthop Trauma Surg*. 2008;128:495–8.
14. Ilayperuma I, Nanayakkara G, Palahepitiya N. Incidence of humeral head of biceps brachii muscle. Anatomical insight. *Int J Morphol*. 2011;29:221–5.
15. Gheno R, Zoner CS, Buck FM, Nico MA, Haghghi P, Trudell DJ, Resnick D. Accessory head of biceps brachii muscle: anatomy, histology, and MRI in cadavers. *AJR Am J Roentgenol*. 2010;194:W80–3.
16. Nakatani T, Tanaka S, Mizukami S. Bilateral four-headed biceps brachii muscles: the median nerve and brachial artery passing through a tunnel formed by a muscle slip from the accessory head. *Clin Anat*. 1998;11:209–12.
17. Crass JR, Van de Vegte GL, Harkavy LA. Tendon echogenicity: ex vivo study. *Radiology*. 1988;167:499–501.
18. Brasseur JL. The biceps tendons: from the top and from the bottom. *J Ultrasound*. 2012;15:29–38.
19. Krzyżanowski W. The use of ultrasound in the assessment of the glenoid labrum of the glenohumeral joint. Part I: ultrasound anatomy and examination technique. *J Ultrason*. 2012;12:164–77.
20. Krzyżanowski W, Tarczyńska M. The use of ultrasound in the assessment of the glenoid labrum of the glenohumeral joint. Part II: examples of labral pathologies. *J Ultrason*. 2012;12:329–41.

21. Tamborrini G, Möller I, Bong D, Miguel M, Marx C, Müller AM, Müller-Gerbl M. The rotator interval: a link between anatomy and ultrasound. *Ultrasound Int Open*. 2017;3:E107–16.
22. Bianchi S, Martinoli C. Shoulder. In: Bianchi S, Martinoli C, editors. *Ultrasound of the musculoskeletal system*. Berlin, Heidelberg, New York: Springer Verlag; 2009. p. 189–332.
23. Chang KV, Chen WS, Wang TG, Hung CY, Chien KL. Associations of sonographic abnormalities of the shoulder with various grades of biceps peritendinous effusion (BPE). *Ultrasound Med Biol*. 2014;40:313–21.
24. Guiffre BM, Lisle DA. Tear of the distal biceps brachii tendon: a new method of ultrasound evaluation. *Australas Radiol*. 2005;49:404–6.
25. Kalume Brigido M, De Maessener M, Jacobson JA, Jamadar DA, Morag Y, Marcellis S. Improved visualization of the radial insertion of the biceps tendon at ultrasound with a lateral approach. *Eur Radiol*. 2009;19:1817–21.
26. Smith J, Finnoff JT, O'Driscoll SW, Lai JK. Sonographic evaluation of the distal biceps tendon using a medial approach: the pronator window. *J Ultrasound Med*. 2010;29:861–5.
27. Keener JD, Brophy RH. Superior labral tears of the shoulder: pathogenesis, evaluation, and treatment. *J Am Acad Orthop Surg*. 2009;17:627–37.
28. Snyder SJ, Karzel RP, Del Pizzo W, Ferkel RD, Friedman MJ. SLAP lesions of the shoulder. *Arthroscopy*. 1990;6:274–9.
29. Modarresi S, Motamedi D, Jude CM. Superior labral anteroposterior lesions of the shoulder: part 2, mechanisms and classification. *AJR Am J Roentgenol*. 2011;197:604–11.
30. Yoo JC, Iyyampillai G, Park D, Koh KH. The influence of bicipital groove morphology on the stability of the long head of the biceps tendon. *J Orthop Surg (Hong Kong)*. 2017;25:2309499017717195.
31. Urita A, Funakoshi T, Amano T, Matsui Y, Kawamura D, Kameda Y, Iwasaki N. Predictive factors of long head of the biceps tendon disorders the bicipital groove morphology and subscapularis tendon tear. *J Shoulder Elbow Surg*. 2016;25:384–9.
32. Habermeyer P, Magosch P, Pritsch M, Scheibel MT, Lichtenberg S. Anterosuperior impingement of the shoulder as a result of pulley lesions: a prospective arthroscopic study. *J Shoulder Elb Surg*. 2004;13:5–12.
33. Bennett WF. Subscapularis, medial, and lateral head coracohumeral ligament insertion anatomy. Arthroscopic appearance and incidence of "hidden" rotator interval lesions. *Arthroscopy*. 2001;17:173–80.
34. Walch G, Nové-Josserand L, Boileau P, Levigne C. Subluxations and dislocations of the tendon of the long head of the biceps. *J Shoulder Elbow Surg*. 1998;7:100–8.
35. Armstrong A, Teeffey SA, Wu T, Clark AM, Middleton WD, Yamaguchi K, Galatz LM. The efficacy of ultrasound in the diagnosis of long head of the biceps tendon pathology. *J Shoulder Elb Surg*. 2006;15:7–11.
36. Read JW, Perko M. Shoulder ultrasound: diagnostic accuracy for impingement syndrome, rotator cuff tear, and biceps tendon pathology. *J Shoulder Elb Surg*. 1998;7:264–71.
37. Farin PU, Jaroma H, Harju A, Soimakallio S. Medial displacement of the biceps brachii tendon: evaluation with dynamic sonography during maximal external shoulder rotation. *Radiology*. 1995;195:845–8.
38. Nho SJ, Strauss EJ, Lenart BA, Provencher MT, Mazzocca AD, Verma NN, Romeo AA. Long head of the biceps tendinopathy: diagnosis and management. *J Am Acad Orthop Surg*. 2010;18:645–56.
39. Patton WC, McCluskey GM III. Biceps tendinitis and subluxation. *Clin Sports Med*. 2001;20:505–29.
40. Favorito PJ, Harding WG III, Heidt RS Jr. Complete arthroscopic examination of the long head of the biceps tendon. *Arthroscopy*. 2001;17:430–2.
41. Boileau P, Ahrens PM, Hatzidakis AM. Entrapment of the long head of the biceps tendon: the hourglass biceps: a cause of pain and locking of the shoulder. *J Shoulder Elb Surg*. 2004;13:249–57.
42. Pujol N, Hargunani R, Gadikoppula S, Holloway B, Ahrens PM. Dynamic ultrasound assessment in the diagnosis of intra-articular entrapment of the biceps tendon (hourglass biceps): a preliminary investigation. *Int J Shoulder Surg*. 2009;3:80–4.
43. Skendzel JG, Jacobson JA, Carpenter JE, Miller BS. Long head of biceps brachii tendon evaluation: accuracy of preoperative ultrasound. *AJR Am J Roentgenol*. 2011;197:942–8.
44. Safran MR, Graham SM. Distal biceps tendon ruptures: incidence, demographics, and the effect of smoking. *Clin Orthop Relat Res*. 2002;404:275–83.
45. Seiler JG III, Parker LM, Chamberland PD, Sherbourne GM, Carpenter WA. The distal biceps tendon. Two potential mechanisms involved in its rupture: arterial supply and mechanical impingement. *J Shoulder Elb Surg*. 1995;4:149–56.
46. Miyamoto RG, Elser F, Millett PJ. Distal biceps tendon injuries. *J Bone Joint Surg Am*. 2010;92:2128–38.
47. Sutton KM, Dodds SD, Ahmad CS, Sethi PM. Surgical treatment of distal biceps rupture. *J Am Acad Orthop Surg*. 2010;18:139–48.
48. McDonald LL, Dewing CC, Shupe LP, Provencher CM. Disorders of the proximal and distal aspects of the biceps muscle. *J Bone Joint Surg Am*. 2013;95:1235–45.
49. O'Driscoll SW, Goncalves LB, Dietz P. The hook test for distal biceps tendon avulsion. *Am J Sports Med*. 2007;35:1865–9.
50. Le Huec JC, Schaefferbeke T, Moinard M, Kind M, Diard F, Dehais J, Le Rebelle A. Traumatic tear of the rotator interval. *J Shoulder Elb Surg*. 1996;5:41–6.
51. de la Fuente J, Blasi M, Martínez S, Barceló P, Cachán C, Miguel M, Pedret C. Ultrasound classification of traumatic distal biceps brachii tendon injuries. *Skeletal Radiol*. 2018;47:519–32.

52. Lobo LD, Fessell DP, Miller BS, Kelly A, Lee JY, Brandon C, Jacobson JA. The role of sonography in differentiating full versus partial distal biceps tendon tears: correlation with surgical findings. *AJR Am J Roentgenol.* 2013;200:158–62.
53. Burke CJ, Adler RS. Ultrasound-guided percutaneous tendon treatments. *AJR Am J Roentgenol.* 2016;207:495–506.
54. Chang KV, Mezian K, Naňka O, Wu WT, Lin CP, Özçakar L. Ultrasound-guided interventions for painful shoulder: from anatomy to evidence. *J Pain Res.* 2018;11:2311–22.
55. Stone TJ, Adler RS. Ultrasound-guided biceps peritendinous injections in the absence of a distended tendon sheath: a novel rotator interval approach. *J Ultrasound Med.* 2015;34:2287–92.
56. Chang KV, Wu SH, Lin SH, Shieh JY, Wang TG, Chen WS. Power Doppler presentation of shoulders with biceps disorder. *Arch Phys Med Rehabil.* 2010;91:624–31.
57. Özçakar L, Kara M, Chang KV, Tekin L, Hung CY, Ulaşlı AM. EURO-MUSCULUS/USPRM basic scanning protocols for shoulder. *Eur J Phys Rehabil Med.* 2015;51:491–6.
58. Gazzillo GP, Finnoff JT, Hall MM, Sayeed YA, Smith J. Accuracy of palpating the long head of the biceps tendon: an ultrasonographic study. *PM&R.* 2011;3:1035–40.
59. Hashiuchi T, Sakurai G, Morimoto M, Komei T, Takakura Y, Tanaka Y. Accuracy of the biceps tendon sheath injection: ultrasound-guided or unguided injection? A randomized controlled trial. *J Shoulder Elb Surg.* 2011;20:1069–73.
60. Zhang J, Ebraheim N, Lause GE. Ultrasound-guided injection for the biceps brachii tendinitis: results and experience. *Ultrasound Med Biol.* 2011;37:729–33.
61. Yiannakopoulos CK, Megaloikonomos PD, Foufa K, Gliatis J. Ultrasound-guided versus palpation-guided corticosteroid injections for tendinosis of the long head of the biceps: a randomized comparative study. *Skelet Radiol.* 2019;12:1–7.
62. Petscavage-Thomas J, Gustas C. Comparison of ultrasound-guided to fluoroscopy-guided biceps tendon sheath therapeutic injection. *J Ultrasound Med.* 2016;35:2217–21.
63. Hufeland M, Wicke S, Verde PE, Krauspe R, Patzer T. Biceps tenodesis versus tenotomy in isolated LHB lesions: a prospective randomized clinical trial. *Arch Orthop Trauma Surg.* 2019;139:961–70.
64. Greditzer HG, Kaplan LD, Lesniak BP, Jose J. Ultrasound-guided percutaneous long head of the biceps tenotomy: a novel technique with case report. *HSS J.* 2014;10:240–4.
65. Aly AR, Rajasekaran S, Mohamed A, Beavis C, Obaid H. Feasibility of ultrasound-guided percutaneous tenotomy of the long head of the biceps tendon – a pilot cadaveric study. *J Clin Ultrasound.* 2015;43:361–6.
66. Atlan F, Werthel JD. Ultrasound-guided intra-articular tenotomy of the long head of the biceps: a cadaveric feasibility study. *Int Orthop.* 2016;40:2567–73.
67. Maree MN, Vrettos BC, Roche SJL, Osch GV. Distal biceps tendinopathy: conservative treatment. *Shoulder Elbow.* 2011;3:104–8.
68. Sanli I, Morgan B, van Tilborg F, Funk L, Gosens T. Single injection of platelet-rich plasma (PRP) for the treatment of refractory distal biceps tendinitis: long-term results of a prospective multicenter cohort study. *Knee Surg Sports Traumatol Arthrosc.* 2016;24:2308–12.
69. Sellon JL, Wempe MK, Smith J. Sonographically guided distal biceps tendon injections: techniques and validation. *J Ultrasound Med.* 2014;33:1461–74.